Stability of a biomembrane tube covered with proteins

Mathijs Janssen,[1,2,*] Susanne Liese,[3,4,†] and Andreas Carlson[1,‡]

[1] *Department of Mathematics, Faculty of Mathematics and Natural Sciences, University of Oslo, 0315 Oslo, Norway*
[2] *Centre for Cancer Cell Reprogramming, Faculty of Medicine, University of Oslo, Montebello, N-0379 Oslo, Norway*
[3] *Max-Planck-Institut für Physik komplexer Systeme, 01187 Dresden, Germany*
[4] *Institute of Physics, University of Augsburg, 86159 Augsburg, Germany*

(Dated: September 29, 2022)

Membrane tubes are essential structural features in cells that help facilitate biomaterial transport and inter- and intracellular signalling. The shape of these tubes can be regulated by the proteins that surround and adhere to them. We study here the stability of a biomembrane tube coated with proteins by combining linear stability analysis and numerical solutions of a Helfrich-like membrane model. Our analysis demonstrates that both long and short wavelength perturbations can destabilise the tubes. Numerical simulations confirm the derived linear stability criteria and also yield the nonlinearly-perturbed vesicle shapes. Our analysis highlights the interplay between the membrane shape and the protein density, where the shape instability concurs with a redistribution of proteins into a banded pattern.

Introduction.— Ubiquitous and essential in biology, lipid membranes are self-assembled fluid films of nanometer thickness that compartmentalize biomaterial and form the boundaries of organelles. These bilayer membranes are much harder to stretch than to bend, which is a property that leads to a wealth of interesting vesicle shapes on mesoscopic lengthscales [1]. In cells, membrane tubes are part of organelles and enable biomaterial exchange, as well as intra- and extra-cellular communication [2, 3]. While some membrane tubes are an integral part of organelles—such as the endoplasmic reticulum, which fills the entire cell interior—other membrane tubes arise transiently [4, 5]. In either case, the interaction between the tube membrane and the surrounding proteins is crucial for its emergence, shaping, and stability [6].

The shapes of lipid bilayers and stability thereof are usually studied through the Helfrich model, which expresses the free energy of a membrane in terms of its Gaussian and mean curvatures [7–10]. Zhong-Can and Helfrich showed that a membrane tube of radius R becomes unstable if the membrane's induced curvature is smaller than $-1/(2R)$ [11, 12]. Likewise, reminiscent of the Rayleigh-Plateau instability of liquid jets, membrane tubes "pearl" when the membrane's surface tension σ drops below $\sigma R^2/\kappa < 3/2$ with κ the membrane's bending rigidity [13–17].

It has been studied how the shapes of membranes are affected by particles—either nearby, attached, or inserted into the membrane—for instance, different types of lipids [18–26], polymers [27–31], nanoparticles [32–36], phospholipid-surfactant mixtures [37], protein pumps [17, 38], adsorbed BAR proteins [39–44], intercalated curvature-inducing proteins [45–47], and crowds of sterically-repelling proteins [48–51] (see also reviews in [52–54]). Generally speaking, the total free energy of such systems contains, beside the Helfrich free energy, the free energy of the particles and a term accounting for the interaction of the membrane with the particles. Expressions for the free energy of the particles often contain terms penalising phase boundaries [19, 37, 39, 45, 55] and terms accounting for interactions between the particles and for entropy, either through a Flory-Huggins theory for a mixture of occupied and unoccupied sites [18, 24, 29, 37, 39], or a Ginzburg-Landau expansion thereof [19, 45, 56]. To describe the interaction of particles with a vesicle, most authors [18, 19, 29, 31, 37, 39, 42, 45–47, 55, 57, 58] considered a linear coupling $\propto \Lambda H \phi$ of the mean curvature H to the areal particle density ϕ with a coupling parameter Λ. Leibler showed that such interaction between proteins and a flat membrane sheet changes its effective bending rigidity to $\kappa - \Lambda^2/a$, with a setting the strength of mutual protein interactions [45]. Consequently, the sheet becomes unstable to ruffles for $\kappa < \Lambda^2/a$.

Experiments have shown that membrane tubes with anchored polymers undergo a pearling instability similar to the tension-induced pearling of uncoated membrane tubes [29]. The experimentally-observed tube shapes were interpreted through a theoretical model based on a free energy description. Surprisingly, it was concluded that the pearl-like shapes have constant mean curvature and areal protein density, although the pearls are connected by narrow necks that would generate a large local mean curvature and significantly contribute to the free energy. One of our aims here is to clarify this instability by deploying a linear stability analysis to analytically predict the onset of the instability, which is complemented and verified by non-linear numerically simulations of the membrane shapes. Given the wealth of cellular processes with membrane tubes, these results have potential relevance to a broad range of cellular processes. Accordingly, we show that the tube's stability criterion is substantially more involved than the earlier-derived

* mathijsj@uio.no
† sliese@pks.mpg.de
‡ acarlson@math.uio.no

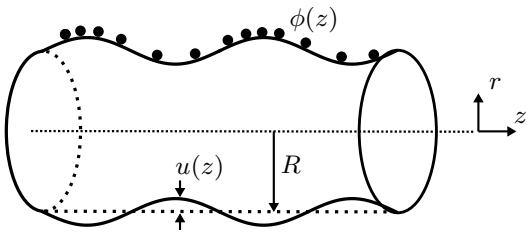

Figure 1. Schematic of a lipid bilayer tube with attached particles. The membrane tube can undergo an instability from a homogeneously coated cylinder of radius R towards an undulating shape $r(z) = R + u(z)$ and varying areal particle density $\phi(z)$.

stability criteria of coated membrane sheets [45] and uncoated membrane tubes [13], and help clarify how proteins segregate on the membrane.

Theory.— We consider a membrane tube and particles that interact with the membrane and among themselves (see Fig. 1). Without loss of generality, from hereon, we refer to these particles as proteins. We partition the total free energy $F = F_H + F_\phi$ into a bare membrane term, given by the Helfrich free energy,

$$F_H = \int \mathrm{d}A \left(2\kappa H^2 + \sigma\right) - P \int \mathrm{d}V \,, \tag{1}$$

and a contribution F_ϕ due to the proteins. In Eq. (1), κ is the bending rigidity, P is the pressure difference between the fluids inside and outside of the tube, σ is the surface tension that acts along the entire membrane, and H is the mean curvature, where our sign convention is such that a cylinder of radius R has $H = -1/(2R)$. In Eq. (1), we omitted a Gaussian bending term, which is topologically invariant [9, 59]. In addition to F_H, we consider the following Ginzburg-Landau free energy for proteins and their interaction with the membrane:

$$F_\phi = \int \mathrm{d}A \Big(- \Lambda\phi H - \mu\phi + \frac{a}{2}\phi^2 + \frac{b}{2}|\nabla\phi|^2 \Big) \,. \tag{2}$$

Here, ϕ is the areal protein density, satisfying $\phi \geq 0$. Moreover, Λ sets the strength of protein-membrane interactions, μ is the binding energy per unit area with which proteins bind to the membrane, a sets the protein-protein interactions, and b sets the cost of phase separating. Throughout, we consider $\Lambda, a, b > 0$, such that the last two terms in Eq. (2) favour a vesicle with a homogenous protein coat. By contrast, the first term in Eq. (2) may lead to undulating ("pearling") tube shapes that minimize the free energy by recruiting proteins (large ϕ) to regions where $H > 0$, while depleting them (small ϕ) from regions where $H < 0$.

Stability analysis (cylindrical tube).— From hereon, we describe the membrane shape using cylindrical coordinates (r, θ, z) and consider a rotationally symmetric tube [17], such that all variables are θ independent. We first study the stability of a membrane tube of length L and fixed radius $r(z) = r$ with a homogeneous coat of proteins at density $\phi(z) = \phi$. In this case, Eqs. (1) and (2) simplify to

$$\frac{F}{\pi L} = \frac{\kappa}{r} + 2r\sigma - Pr^2 + \Lambda\phi - 2r\mu\phi + a\phi^2 r \,. \tag{3}$$

For the free energy $F(r, \phi)$ to be in a local minimum at a given $r = R$ and $\phi = \Phi$, three conditions must be met. First, minimizing Eq. (3) with respect to the protein density $[(\partial F/\partial\phi)_{R,\Phi} = 0]$ yields

$$\mu = a\Phi + \frac{\Lambda}{2R} \,, \tag{4}$$

which means that, unlike a membrane sheet [45], a membrane tube has a finite protein density $\Phi \neq 0$ if $\mu = 0$. Second, minimizing Eq. (3) with respect to the vesicle radius $[(\partial F/\partial r)_{R,\Phi} = 0]$ yields

$$\frac{PR^3}{\kappa} = \frac{\sigma R^2}{\kappa} - \frac{1}{2} - \frac{a\Phi^2 R^2}{2\kappa} - \frac{\Lambda\Phi R}{2\kappa} \,, \tag{5}$$

where we used Eq. (4) to eliminate μ. While the first two terms on the right-hand side of Eq. (5) represent the conventional Laplace pressure, the last two terms are new and specific to our model problem. Note that, by fixing the tube length L, we assume to have (indirect) control over the membrane tension σ. By contrast, the pressure P adjust itself for given R, σ, and other parameters according to Eq. (5).

Finally, for the tube to be stable, the Hessian determinant of F must be positive. This amounts to $\Big[(\partial^2 F/\partial\phi^2)(\partial^2 F/\partial r^2) - \big(\partial^2 F/\partial\phi\partial r\big)^2\Big]_{R,\Phi} > 0$, giving

$$\frac{PR^3}{\kappa} < 1 - \frac{\Lambda^2}{4\kappa a} \,. \tag{6}$$

From Eqs. (5) and (6) we conclude that the coated cylinder is stable if

$$\frac{\sigma R^2}{\kappa} < \frac{3}{2} + \frac{a\Phi^2 R^2}{2\kappa} + \frac{\Lambda\Phi R}{2\kappa} - \frac{\Lambda^2}{4\kappa a} \,. \tag{7}$$

Equation (7) generalizes a well-known stability criterion $\sigma R^2/\kappa < 3/2$ for uncoated membrane tubes [8, 15–17], adding three terms related to the attached proteins. Summarising, for given σ, Λ, μ and a, a tube of constant radius R has a coat of density Φ [Eq. (4)] and a pressure drop P [Eq. (5)] across its membrane.

Linear Stability Analysis.— To study what happens to the tube if Eq. (7) is not satisfied, we now consider a tube with slight undulations in its radius and coat density, $r(z) = R + u(z)$ and $\phi(z) = \Phi + \varphi(z)$, with $u(z) \ll R$ and $\varphi(z) \ll \Phi$ (see Fig. 1). We use that $\sqrt{g} = r\sqrt{1 + (\partial_z r)^2}$, with g being the metric determinant (and with $\partial_z = \partial/\partial z$), and that [17, 60, 61]

$$2H = \frac{1}{\sqrt{1 + (\partial_z r)^2}} \left(\frac{\partial_z^2 r}{1 + (\partial_z r)^2} - \frac{1}{r} \right) \,. \tag{8}$$

Using the scaling—throughout, barred variables are dimensionless—$\bar{F} = F/(2\pi\kappa)$, $\bar{z} = z/R$, $\bar{L} = L/R$, $\bar{r} = r/R$, $\bar{\phi}(z) = \phi/\Phi$, $\bar{\sigma} = \sigma R^2/\kappa$, $\bar{P} = PR^3/\kappa$, $\bar{\Lambda} = \Lambda\Phi R/\kappa$, $\bar{a} = a\Phi^2R^2/\kappa$, $\bar{\mu} = \mu\Phi R^2/\kappa$ and $\bar{b} = b\Phi^2/\kappa$, we find $\bar{F} = \bar{F}_H + \bar{F}_\phi$ with

$$\bar{F}_H = \frac{1}{2}\int_0^{\bar{L}} \mathrm{d}\bar{z} \left\{ \frac{\bar{r}}{\sqrt{1+(\partial_{\bar{z}}\bar{r})^2}} \left(\frac{\partial_{\bar{z}}^2\bar{r}}{1+(\partial_{\bar{z}}\bar{r})^2} - \frac{1}{\bar{r}} \right)^2 + 2\bar{\sigma}\bar{r}\sqrt{1+(\partial_{\bar{z}}\bar{r})^2} - \bar{P}\bar{r}^2 \right\}, \tag{9a}$$

$$\bar{F}_\phi = \frac{1}{2}\int_0^{\bar{L}} \mathrm{d}\bar{z} \left\{ \bar{r}\sqrt{1+(\partial_{\bar{z}}\bar{r})^2}\left[-2\bar{\mu}\bar{\phi} + \bar{a}\bar{\phi}^2 + \bar{b}(\partial_{\bar{z}}\bar{\phi})^2\right] - \bar{\Lambda}\bar{\phi}\left(\frac{\bar{r}\partial_{\bar{z}}^2\bar{r}}{1+(\partial_{\bar{z}}\bar{r})^2} - 1 \right) \right\}. \tag{9b}$$

Next, we expand the perturbations $\bar{u}(\bar{z}) = u/R$ and $\bar{\varphi}(\bar{z}) = \varphi/\Phi$ into Fourier modes,

$$\bar{u} = \sum_{\bar{q}\neq 0} \bar{u}_{\bar{q}} \mathrm{e}^{\mathrm{i}\bar{q}\bar{z}}, \qquad \bar{\varphi} = \sum_{\bar{q}\neq 0} \bar{\phi}_{\bar{q}} \mathrm{e}^{\mathrm{i}\bar{q}\bar{z}}, \tag{10}$$

where $\bar{q} = 2\pi n/\bar{L}$ are dimensionless wave numbers (with $n \in \mathbb{N}$) and where $\bar{u}_{\bar{q}}$ and $\bar{\phi}_{\bar{q}}$ are the amplitudes of the modes. If volume conservation is imposed, the amplitudes $\bar{u}_{\bar{q}}$ are constrained relative to each other. Inserting $\bar{r}(\bar{z}) = 1 + \bar{u}(\bar{z})$ into $\bar{F}_H$ leads to (see Refs. [15–17, 61] and the Supplemental Material [62])

$$\bar{F}_H = \frac{\bar{L}}{4}\sum_{\bar{q}\neq 0} \bar{u}_{\bar{q}}\bar{u}_{-\bar{q}} \left\{ 2\bar{q}^4 + \bar{q}^2(2\bar{\sigma}-1) + 2 - 2\bar{P} \right\}. \tag{11}$$

Likewise, inserting Eq. (10) into $\bar{F}_\phi$ and retaining quadratic terms gives [62]

$$\bar{F}_\phi = \frac{\bar{L}}{4}\sum_{\bar{q}\neq 0} \left\{ \bar{q}^2(\bar{\Lambda}-\bar{a})\,\bar{u}_{\bar{q}}\bar{u}_{-\bar{q}} + 2\bar{\Lambda}(\bar{q}^2-1)\,\bar{u}_{\bar{q}}\bar{\phi}_{-\bar{q}} + 2(\bar{a}+\bar{b}\bar{q}^2)\,\bar{\phi}_{\bar{q}}\bar{\phi}_{-\bar{q}} \right\}. \tag{12}$$

Combining Eqs. (11) and (12) and inserting $\bar{P}$ from Eq. (5), we find

$$\bar{F} = \frac{\bar{L}}{4}\sum_{\bar{q}\neq 0} \begin{pmatrix} \bar{u}_{\bar{q}} & \bar{\phi}_{\bar{q}} \end{pmatrix} \underbrace{\begin{pmatrix} 2\bar{q}^4 + \zeta_2\bar{q}^2 + \zeta_0 & \bar{\Lambda}(\bar{q}^2-1) \\ \bar{\Lambda}(\bar{q}^2-1) & 2(\bar{a}+\bar{b}\bar{q}^2) \end{pmatrix}}_{\equiv A} \begin{pmatrix} \bar{u}_{-\bar{q}} \\ \bar{\phi}_{-\bar{q}} \end{pmatrix}, \tag{13}$$

with $\zeta_2 = \bar{\Lambda} - \bar{a} + 2\bar{\sigma} - 1$ and $\zeta_0 = \bar{\Lambda} + \bar{a} - 2\bar{\sigma} + 3$.

Considering Eq. (13) in the limit $R \to \infty$, we found (see Ref. [62]) a leading order contribution at $\mathcal{O}(R^2)$ coinciding with the free energy of a ruffled membrane sheet, studied previously by Leibler [45]. Away from that limit, Eq. (13) is much more involved, though, the chief reason lying in the different expansions of the square root of the metric determinant: a sheet with small ruffles of height h yields, in the Mongé parameterisation, $\sqrt{g} \approx 1 + (\nabla h)^2/2 + \mathcal{O}(h^3)$; the ruffled tube in arc-length parametrisation yielded $\sqrt{g} = r\sqrt{1+(\partial_z r)^2} \approx R + u + R(\partial_z u)^2/2 + \mathcal{O}(u^3)$ instead. The presence of terms linear in the perturbation in the arc-length parametrisation (and their absence in the Mongé parameterisation) precipitates in many more terms at quadratic order in the analysis of the membrane tube.

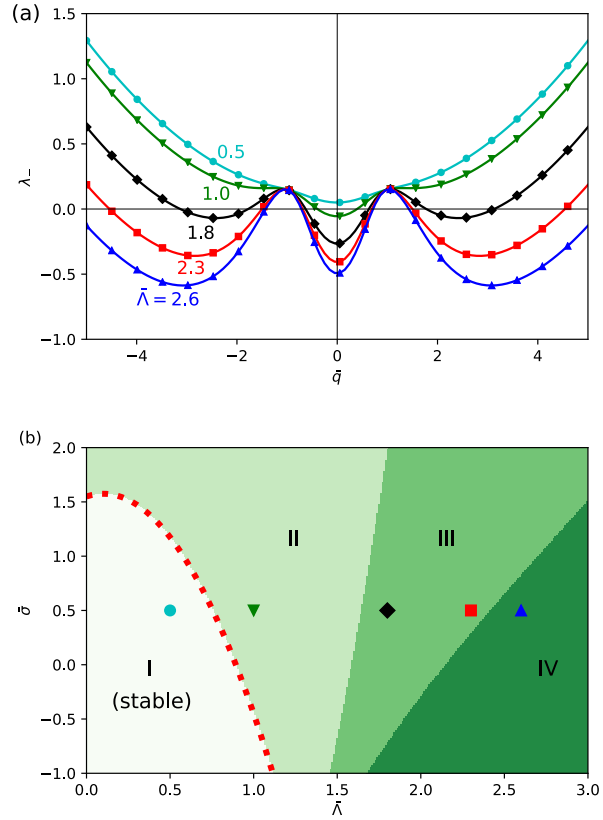

Figure 2. (a) The smallest eigenvalue λ_- of A [Eq. (13)] for $\bar{a} = 0.1$, $\bar{b} = 0.05$, $\bar{\sigma} = 0.5$, and $\bar{\Lambda} = [0.5, 1.0, 1.8, 2.3, 2.6]$. In (a), we discern four different types of minima of λ_-, which we denote with roman numerals: I, where $\lambda_- > 0$ for all q; II, where $\min(\lambda_-) < 0$ at $q = 0$ is the only minimum for which $\lambda_- < 0$; III, same as II, but with a secondary minimum for which $\lambda_- < 0$ for $q \neq 0$, and; IV, where $\min(\lambda_-) < 0$ at $q \neq 0$. In panel (b), we characterize the minima of λ_- according to these four cases in the plane of $\bar{\sigma}$ and $\bar{\Lambda}$. Symbols correspond to the parameter settings used in panel (a). The red dotted line represents Eq. (7).

The stability of the coated membrane tube is governed by the smallest eigenvalue $\lambda_- = \mathrm{Tr}(A)/2 - \sqrt{\mathrm{Tr}(A)^2/4 - \det(A)}$ of A [Eq. (13)], where $\mathrm{Tr}(A)$ and $\det(A)$ are the trace and determinant of A. When $\lambda_- < 0$, the system is unstable to a combination of density and radius perturbations set by the elements of the corresponding eigenvector. Figure 2(a) shows λ_- for $\bar{a} = 0.1$, $\bar{b} = 0.05$, $\bar{\sigma} = 0.5$, and several $\bar{\Lambda}$ as indicated. We observe local minima at $\bar{q} = 0$ for all considered $\bar{\Lambda}$

and for finite $\bar{q}$ in a few cases; these minima appear, depending on $\bar{\Lambda}$, both at positive and negative λ_- values. We discern four cases: for $\bar{\Lambda} = 0.5$, $\lambda_- > 0$ for all q (case I); for $\bar{\Lambda} = 1.0$, λ_- is negative only around $q = 0$ (case II); for $\bar{\Lambda} = 1.8$ and 2.3, λ_- has a negative global minimum at $q = 0$ and a negative local minimum for $q \neq 0$ (case III); and for $\bar{\Lambda} = 2.6$, λ_- has a negative global minimum at $q \neq 0$ and a negative local minimum for $q = 0$ (case IV). In Fig. 2(b) we characterize λ_- according to the above cases in the plane of $\bar{\sigma}$ and $\bar{\Lambda}$. At the boundary between cases I and II, the minimum of λ_- at $\bar{q} = 0$ crosses zero. $\lambda_- = 0$ requires $\det(A) = 0$ which, after setting $\bar{q} = 0$ in A, gives the stability criterion Eq. (7) in dimensionless form, $2\bar{\sigma} = \left(3 + \bar{a} + \bar{\Lambda} - \bar{\Lambda}^2/2\bar{a}\right)$. We indicate this analytical result with a red dotted line. It would be interesting to also characterise the boundary between cases II and III, where the local minimum of λ_- at $\bar{q} \neq 0$ crosses zero, as this is the criterion for finite-wavelength undulations to become unstable. In this case, $\det(A) = 0$ is a sixth-order polynomial in $\bar{q}$ containing only even powers of $\bar{q}$, which can thus be written as a cubic polynomial, $\det(A) = \alpha x^3 + \beta x^2 + \gamma x + \delta$, with $x = \bar{q}^2$, $\alpha = \bar{b}$, $\beta = \bar{b}\zeta_2 + \bar{a} - \bar{\Lambda}^2/4$, $\gamma = \bar{a}\zeta_2 + \bar{b}\zeta_0 + \bar{\Lambda}^2/2$, and $\delta = \bar{a}\zeta_0 - \bar{\Lambda}^2/4$. Depending on the sign of the discriminant $\Delta = \beta^2\gamma^2 - 4\alpha\gamma^3 - 4\beta^3\delta - 27\alpha^2\delta^2 + 18\alpha\beta\gamma\delta$, $\det(A) = 0$ thus has either 1 (if $\Delta < 0$) or 3 (if $\Delta > 0$) real solutions. While these expressions allow us to analytically express the stability of the protein-covered membrane, the resulting expressions are not tractable.

Energy Minimizing Shape.— Next, we discuss the membrane shape beyond the onset of the instability. If an instability is found for $q \neq 0$ the membrane adopts an undulating shape, which in a minimal form is approximated by

$$\bar{r}(\bar{z}) = \bar{r}_0 + \overline{\Delta r}\sin(\bar{q}\bar{z})\,, \tag{14a}$$

$$\bar{\phi}(\bar{z}) = \bar{\phi}_0 + \overline{\Delta\phi}\sin(\bar{q}\bar{z})\,, \tag{14b}$$

where we set $\bar{r}_0 = \sqrt{1 - \overline{\Delta r}^2/2}$ to impose volume conservation. We insert Eq. (14) into the free energy [Eq. (9)], which we then minimize—for given $\bar{a}, \bar{b}, \bar{\sigma}$, and $\bar{\Lambda}$—with respect to $\overline{\Delta r}$, $\bar{\phi}_0$, and $\overline{\Delta\phi}$. This mimimization is subject to the constraint $|\overline{\Delta\phi}| \leq \bar{\phi}_0$ to ensure that $\bar{\phi} \geq 0$. We note that, as the shapes Eq. (14) conserve volume by construction, we can omit the constant term $-P\int \mathrm{d}V$ from Eq. (1). Figure 3(a) shows the free energy difference between an undulating and a straight membrane tube as a function of the wave number $\bar{q}$ for different $\bar{\Lambda}$ and $\bar{\sigma} = 0.5$, $\bar{a} = 0.1$, and $\bar{b} = 0.05$. In line with the stability analysis (cf. Fig. 2), $\Delta\bar{F}$ displays minima for $\bar{q} = 0$ and $\bar{q} \neq 0$. Here, $\bar{q} = 0$ corresponds to a shape undulation of the length of the vesicle. In contrast, for $\bar{q} \neq 0$, the wave length is finite, corresponding to undulating shapes. Figure 3(b) shows the straight tube ($\bar{r} = 1$) as well as three energy-minimizing undulating shapes, together with their areal density $\bar{\phi}$ and local mean curvature $\bar{h} = RH$ as colormaps. While the energy-minimizing vesicles have only small-amplitude undulations in their shape ($\overline{\Delta r} < \bar{r}_0$), their areal density $\bar{\phi}(\bar{z})$ varies strongly: between zero and a value much beyond $\bar{\phi} = 1$ of a homogenously-coated straight membrane tube. As anticipated, for this large protein-membrane interaction (large $\bar{\Lambda}$) and weak mutual protein interaction and phase boundary penalty (small $\bar{a}$ and $\bar{b}$), the system minimizes its free energy through a pearling shape where the necks (where $\bar{h} > 0$) recruit proteins and the bulbs (where

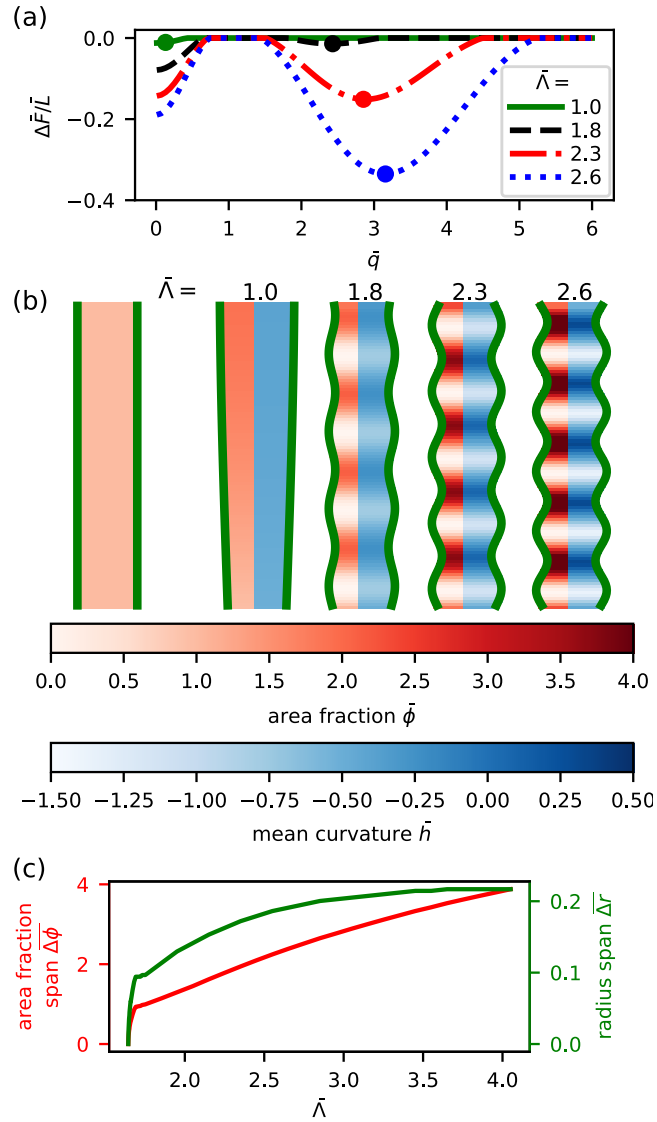

Figure 3. (a) Free energy difference $\Delta\bar{F}$ between an undulating and a straight membrane tube vs. the wave number $\bar{q}$ for four $\bar{\Lambda}$ as indicated. The membrane shape is approximated by Eq. (14). (b) Cylindrical shape with $\bar{r} = 1$ and $\bar{\phi} = 1$ and four undulating shapes that correspond to $\bar{\Lambda}$ and $\bar{q}$ value indicated by dots in panel (a). The cylindrical shape has a constant mean curvature $\bar{h} = -1/2$ and a constant protein density $\bar{\phi} = 1$. For the undulating shapes the space-dependent areal protein density and mean curvature are shown as colormaps. (c) Amplitude of the radius and areal protein density vs. $\bar{\Lambda}$. We used $\bar{\sigma} = 0.5$, $\bar{a} = 0.1$, $\bar{b} = 0.05$ in all panels.

$\bar{h} < 0$) repel them. Figure 3(c) shows the amplitudes of the radius ($\overline{\Delta r}$) and the areal protein density ($\overline{\Delta\phi}$) vs. $\bar{\Lambda}$. We see that $\overline{\Delta r}$ saturates to $\overline{\Delta r} \approx 0.22$ for large $\bar{\Lambda}$. Conversely, $\overline{\Delta\phi}$ increases roughly linearly with $\bar{\Lambda}$ beyond $\bar{\Lambda} = 1.7$.

We note the undulating shapes found in Fig. 3 and anticipated in Fig. 2 are characteristic for the small $\bar{a}$ and $\bar{b}$ used there. For larger $\bar{a}$ and $\bar{b}$, the negative local minima for $\bar{q} \neq 0$ do not appear in the same $\bar{\sigma}$ and $\bar{\Lambda}$ range [62]. Physically, in order for particles to incite a membrane tube instability, these particles need to interact strongly with the membrane, but not among themselves.

Conclusion.— We studied the stability of a membrane tube coated with proteins. We performed a linear stability analysis and analytically determined a criterion [Eq. (7)] for the long wavelength instability. We characterised the finite wavelength instability through numerical calculations. The onset of both instabilities is determined by both membrane and protein parameters. Proteins thus have a regulatory effect on the shape and stability of membrane tubes. Our model revealed an interplay between membrane shape and protein density: the membrane shape instability studied here concurred with a redistribution of proteins into a banded pattern. We hope that these results inspire experiments seeking protein bands on membrane tubes. Future work may also extend our analysis to noncylindrically symmetric tubes, or track the out-of-equilibrium instability, where the $q = 0$ modes may be damped hydrodynamically, favouring the $q \neq 0$ modes [17].

Acknowledgement.— We thank Sami Al-Izzi, David Andelman, Andrew Callan-Jones, and Markus Deserno for insightful discussions. The research leading to these results has received funding from the European Union's Horizon 2020 research and innovation programme under the Marie Skłodowska-Curie grant agreement No 801133. MJ was supported by an Advanced Grant from the European Research Council (no. 788954).

[1] U. Seifert, Advances in Physics **46**, 13 (1997).
[2] M. Drab, D. Stopar, V. Kralj-Iglič, and A. Iglič, Cells **8**, 626 (2019).
[3] J. Hurtig, D. T. Chiu, and B. Önfelt, WIREs Nanomedicine and Nanobiotechnology **2**, 260 (2010).
[4] J. Nixon-Abell, C. J. Obara, A. V. Weigel, D. Li, W. R. Legant, C. S. Xu, H. A. Pasolli, K. Harvey, H. F. Hess, E. Betzig, C. Blackstone, and J. Lippincott-Schwartz, Science **354**, aaf3928 (2016).
[5] J. F. Presley, N. B. Cole, T. A. Schroer, K. Hirschberg, K. J. M. Zaal, and J. Lippincott-Schwartz, Nature **389**, 81 (1997).
[6] P. Bassereau, R. Jin, T. Baumgart, M. Deserno, R. Dimova, V. A. Frolov, P. V. Bashkirov, H. Grubmüller, R. Jahn, H. J. Risselada, L. Johannes, M. M. Kozlov, R. Lipowsky, T. J. Pucadyil, W. F. Zeno, J. C. Stachowiak, D. Stamou, A. Breuer, L. Lauritsen, C. Simon, C. Sykes, G. A. Voth, and T. R. Weikl, Journal of Physics D: Applied Physics **51**, 343001 (2018).
[7] W. Helfrich, Zeitschrift für Naturforschung C **28**, 693 (1973).
[8] T. R. Powers, Reviews of Modern Physics **82**, 1607 (2010).
[9] M. Deserno, Chemistry and physics of lipids **185**, 11 (2015).
[10] J. Guven and P. Vázquez-Montejo, in *The Role of Mechanics in the Study of Lipid Bilayers* (Springer, 2018) pp. 167–219.
[11] O.-Y. Zhong-Can and W. Helfrich, Physical Review A **39**, 5280 (1989).
[12] S. Chaïeb and S. Rica, Phys. Rev. E **58**, 7733 (1998).
[13] R. Bar-Ziv and E. Moses, Phys. Rev. Lett. **73**, 1392 (1994).
[14] D. Jan Bukman, J. Hua Yao, and M. Wortis, Phys. Rev. E **54**, 5463 (1996).
[15] K. Gurin, V. Lebedev, and A. Muratov, Journal of Experimental and Theoretical Physics **83**, 321 (1996).
[16] R. E. Goldstein, P. Nelson, T. Powers, and U. Seifert, Journal de Physique II **6**, 767 (1996).
[17] S. C. Al-Izzi, G. Rowlands, P. Sens, and M. S. Turner, Phys. Rev. Lett. **120**, 138102 (2018).
[18] V. Markin, Biophysical Journal **36**, 1 (1981).
[19] S. Leibler and D. Andelman, Journal de physique **48**, 2013 (1987).
[20] T. Kawakatsu, D. Andelman, K. Kawasaki, and T. Taniguchi, Journal de Physique II **3**, 971 (1993).
[21] T. Taniguchi, K. Kawasaki, D. Andelman, and T. Kawakatsu, Journal de Physique II **4**, 1333 (1994).
[22] T. Taniguchi, Phys. Rev. Lett. **76**, 4444 (1996).
[23] P. B. S. Kumar and M. Rao, Phys. Rev. Lett. **80**, 2489 (1998).
[24] S. Givli, H. Giang, and K. Bhattacharya, SIAM Journal on Applied Mathematics **72**, 489 (2012).
[25] S. Katz and S. Givli, Computational and mathematical methods in medicine **2017**, 10.1155/2017/7275131 (2017).
[26] P. Nowakowski, B. H. Stumpf, A.-S. Smith, and A. Maciołek, arxiv:2206.03424 (2022).
[27] V. Frette, I. Tsafrir, M.-A. Guedeau-Boudeville, L. Jullien, D. Kandel, and J. Stavans, Physical review letters **83**, 2465 (1999).
[28] M. Breidenich, R. Netz, and R. Lipowsky, EPL (Europhysics Letters) **49**, 431 (2000).
[29] I. Tsafrir, D. Sagi, T. Arzi, M.-A. Guedeau-Boudeville, V. Frette, D. Kandel, and J. Stavans, Phys. Rev. Lett. **86**, 1138 (2001).
[30] F. Campelo and A. Hernandez-Machado, The European Physical Journal Special Topics **143**, 101 (2007).
[31] F. Campelo and A. Hernández-Machado, Phys. Rev. Lett. **99**, 088101 (2007).
[32] R. R. Netz and P. Pincus, Physical Review E **52**, 4114 (1995).
[33] R. Lipowsky and H.-G. Döbereiner, EPL (Europhysics Letters) **43**, 219 (1998).
[34] H. Noguchi and M. Takasu, Biophysical journal **83**, 299 (2002).
[35] M. Deserno, Phys. Rev. E **69**, 031903 (2004).
[36] I. Palaia, A. Paraschiv, V. E. Debets, C. Storm, and

A. Šarić, ACS Nano **15**, 15794 (2021).
[37] D. Andelman, M. Kozlov, and W. Helfrich, EPL (Europhysics Letters) **25**, 231 (1994).
[38] S. Ramaswamy, J. Toner, and J. Prost, Physical review letters **84**, 3494 (2000).
[39] A. Veksler and N. S. Gov, Biophysical journal **93**, 3798 (2007).
[40] T. Auth and G. Gompper, Phys. Rev. E **80**, 031901 (2009).
[41] D. Kabaso, N. Bobrovska, W. Góźdź, N. Gov, V. Kralj-Iglič, P. Veranič, and A. Iglič, Journal of biomechanics **45**, 231 (2012).
[42] N. Gov, Philosophical Transactions of the Royal Society B: Biological Sciences **373**, 20170115 (2018).
[43] C. Tozzi, N. Walani, and M. Arroyo, New journal of physics **21**, 093004 (2019).
[44] M. Fošnarič, S. Penič, A. Iglič, V. Kralj-Iglič, M. Drab, and N. S. Gov, Soft Matter **15**, 5319 (2019).
[45] S. Leibler, Journal de Physique **47**, 507 (1986).
[46] J. Derganc, Physical Biology **4**, 317 (2007).
[47] H. Noguchi, Soft Matter **17**, 10469 (2021).
[48] J. C. Stachowiak, E. M. Schmid, C. J. Ryan, H. S. Ann, D. Y. Sasaki, M. B. Sherman, P. L. Geissler, D. A. Fletcher, and C. C. Hayden, Nature cell biology **14**, 944 (2012).
[49] M. Lindén, P. Sens, and R. Phillips, PLoS computational biology **8**, e1002431 (2012).
[50] S. Liese, E. M. Wenzel, I. Kjos, R. R. Molina, S. W. Schultz, A. Brech, H. Stenmark, C. Raiborg, and A. Carlson, Proceedings of the National Academy of Sciences **117**, 28614 (2020).
[51] S. Liese and A. Carlson, Biophysical Journal **120**, 2482 (2021).
[52] J. Zimmerberg and M. M. Kozlov, Nature reviews Molecular cell biology **7**, 9 (2006).
[53] M. Schulz, A. Olubummo, and W. H. Binder, Soft Matter **8**, 4849 (2012).
[54] H. Alimohamadi and P. Rangamani, Biomolecules **8**, 120 (2018).
[55] R. Capovilla and J. Guven, Journal of Physics: Condensed Matter **16**, S2187 (2004).
[56] J. Klebes, P. Clegg, and R. M. L. Evans, Phys. Rev. E **105**, 064802 (2022).
[57] A. Callan-Jones and P. Bassereau, Current Opinion in Solid State and Materials Science **17**, 143 (2013).
[58] M. Naoz and N. S. Gov, Cells **9**, 782 (2020).
[59] F. Jülicher and R. Lipowsky, Phys. Rev. E **53**, 2670 (1996).
[60] M. Deserno, Notes on differential geometry (2004).
[61] J. Tchoufag, A. Sahu, and K. K. Mandadapu, Phys. Rev. Lett. **128**, 068101 (2022).
[62] See Supplemental Material at ... for a list of used symbols, for Fig. 2, replotted for larger $\bar{a}$ and $\bar{b}$, for a discussion of instabilities of membrane sheets, and for a derivation of Eqs. (11) and (12).